Rab35 regulates phagosome formation through recruitment of ACAP2 in macrophages during FcγR-mediated phagocytosis

Youhei Egami[1], Mitsunori Fukuda[2] and Nobukazu Araki[1,*]

[1]Department of Histology and Cell Biology, School of Medicine, Kagawa University, Miki, Kagawa 761-0793, Japan
[2]Laboratory of Membrane Trafficking Mechanisms, Department of Developmental Biology and Neurosciences, Graduate School of Life Sciences, Tohoku University, Aobayama, Aoba-ku, Sendai, Miyagi 980-8578, Japan
*Author for correspondence (naraki@med.kagawa-u.ac.jp)

Accepted 8 June 2011
Journal of Cell Science 124, 3557–3567

doi: 10.1242/jcs.083881

Summary

Phagosome formation and subsequent maturation are complex sequences of events that involve actin cytoskeleton remodeling and membrane trafficking. Here, we demonstrate that the Ras-related protein Rab35 is involved in the early stage of FcγR-mediated phagocytosis in macrophages. Live-cell image analysis revealed that Rab35 was markedly concentrated at the membrane where IgG-opsonized erythrocytes (IgG-Es) are bound. Rab35 silencing by RNA interference (RNAi) or the expression of GDP- or GTP-locked Rab35 mutant drastically reduced the rate of phagocytosis of IgG-Es. Actin-mediated pseudopod extension to form phagocytic cups was disturbed by the Rab35 silencing or the expression of GDP-Rab35, although initial actin assembly at the IgG-E binding sites was not inhibited. Furthermore, GTP-Rab35-dependent recruitment of ACAP2, an ARF6 GTPase-activating protein, was shown in the phagocytic cup formation. Concomitantly, overexpression of ACAP2 along with GTP-locked Rab35 showed a synergistic inhibitory effect on phagocytosis. It is likely that Rab35 regulates actin-dependent phagosome formation by recruiting ACAP2, which might control actin remodeling and membrane traffic through ARF6.

Key words: ACAP2, Rab35, Actin cytoskeleton, Live-cell imaging, Macrophages, Phagocytosis

Introduction

Phagocytosis is a specialized form of endocytosis that allows the ingestion of large particles (>1 μm in diameter), and has a crucial role in innate immunity and tissue remodeling. Professional phagocytes, mainly macrophages and neutrophils, are equipped for ingesting foreign particles, invading microorganisms and apoptotic bodies, contributing to the resolution of infections and the clearance of senescent or damaged cells. Phagocytosis of a particle is initiated by the binding of that particle to a specific cell surface receptor, including Fcγ receptors (FcγRs), complement receptors, scavenger receptors and Toll-like receptors (Greenberg and Grinstein, 2002). Phagocytosis through FcγRs, which is the best characterized, is accompanied by actin polymerization and reorganization, which drive the formation of phagocytic cups around IgG-opsonized particles (Araki et al., 2003; Araki et al., 1996; Groves et al., 2008; Swanson, 2008). The regulation of actin polymerization and reorganization during phagocytic cup formation has been shown to depend on Rho-family GTPases, such as Rac1 and Cdc42 (Beemiller et al., 2010; Caron and Hall, 1998; Castellano et al., 2000; Cox et al., 1997; Massol et al., 1998). In their active GTP-bound conformation, these proteins interact with and activate downstream effectors, which are directly involved in the regulation of actin filament assembly proteins, such as Wiskott-Aldrich syndrome protein (WASP) (Castellano et al., 2001; Coppolino et al., 2001; Park and Cox, 2009). It is noteworthy that GTP-bound Cdc42 accelerates the actin-nucleating activity of the Arp2/3 complex through the direct binding of WASP (Higgs and Pollard, 2001; Takenawa and Miki, 2001), providing a nidus for the formation of an actin polymer network. Arp2/3-mediated actin assembly is proposed to generate the force necessary to push the plasma membrane and thus create cell surface protrusions or phagocytic cups (May et al., 2000; May and Machesky, 2001). Concomitantly, actin remodeling and disassembly at the base of phagocytic cups also take place to complete phagosome formation. After the closure of the phagocytic cups, the newly formed phagosomes mature by a series of interactions with endocytic compartments, eventually fusing with lysosomes and effecting particle degradation (Downey et al., 1999; Vieira et al., 2002).

Rab proteins form the largest group within the Ras superfamily of low molecular weight GTPases that function as molecular switches by cycling between their inactive GDP- and active GTP-bound forms (Pereira-Leal and Seabra, 2001; Stenmark, 2009; Zerial and McBride, 2001). The inactive GDP-bound forms are thought to be quiescent in the cytoplasm and complexed with their chaperone Rab-GDIs. Conversely, the active GTP-bound forms physically interact with effectors on membranes and influence critical steps in membrane trafficking. To date, a number of Rab proteins have been shown to have roles in vesicle formation, motility, docking and fusion (Fukuda, 2008; Grosshans et al., 2006; Jordens et al., 2005; Schwartz et al., 2007). Rab35, a member of the Rab GTPase family, is localized on the plasma membrane and some endocytic compartments, and

controls a fast endocytic recycling pathway (Kouranti et al., 2006). A recent study has shown that Rab35 functions downstream of clathrin and upstream of Rab7, and acts synergistically with a recycling regulator, Rab11, in the nematode (Sato et al., 2008). Besides its roles in regulating receptor-mediated endocytosis, Rab35 has been shown to interact with the phagosomal membrane and to control phagosome–lysosome fusion in macrophages (Smith et al., 2007). It was also reported that Rab35 was involved in Cdc42 and Rac1 transport during phagocytosis in *Drosophila* cells (Shim et al., 2010), although the precise molecular mechanism is unknown.

Although not much is known about the downstream effectors of Rab35, it was recently found that Rab35 binds fascin and regulates actin bundling (Zhang et al., 2009). Most recently, ACAP2 (also known as centaurin β2) has been identified as a novel Rab35-binding protein (Kanno et al., 2010). Because ACAP2 is an ADP-ribosylation factor (ARF) 6 GTPase-activating protein (GAP), ACAP2 modulates Rab35-dependent neurite outgrowth of PC12 cells through ARF6 (Kanno et al., 2010). Importantly, ARF6 is known to be involved in the regulation of membrane traffic and actin remodeling in FcγR-mediated phagocytosis (Niedergang et al., 2003; Zhang et al., 1998). However, in the case of phagocytosis, upstream regulators of ARF6 have not been clarified. Therefore, it is of interest to clarify the functional link between Rab35 and ACAP2 with reference to the regulation of ARF6 GTPase activity in FcγR-mediated phagocytosis.

In the present study, we focused on the role of Rab35 in the early stage of FcγR-mediated phagocytosis rather than in phagosome maturation, because Rab35 was predominantly observed on the membrane of forming phagosomes in macrophages. This study yielded novel insights into the function of Rab35 in phagosome formation; based on our results, we believe that Rab35 regulates coordinated remodeling of the actin cytoskeleton and/or membrane architecture by recruiting ACAP2, a GAP for ARF6 GTPase, in the process of the phagosome formation.

Results

Rab35 is recruited to the phagocytic membrane at an early stage of phagosome formation

Although Rab35 has been shown to associate with the phagosomal membrane and to regulate phagosome maturation (Smith et al., 2007), it remains unclear whether Rab35 is involved in the early stage of FcγR-mediated phagocytosis. To investigate the Rab35 dynamics during the early stage of phagosome formation, the internalization of IgG-opsonized erythrocytes (IgG-Es) was observed by time-lapse fluorescence microscopy in live RAW264 macrophages expressing GFP–Rab35. Before to the onset of phagocytosis, GFP–Rab35 was largely observed in the cytosol, and was also associated with the plasma membrane and some intracellular vesicles in some degree, as previously shown in other cell types (Kouranti et al., 2006; Patino-Lopez et al., 2008). After adding IgG-Es to the cells, more GFP–Rab35 appeared to be recruited to the sites of IgG-E binding. Of note, Rab35 was predominately localized on the membranes of extending pseudopodia or phagocytic cups along the surface of IgG-Es (Fig. 1 and supplementary material Movie 1). Coexpression of GFP–Rab35 with CFP–Lamp1 demonstrated that the recruitment of Rab35 to the phagocytic membranes occurred much earlier than that of Lamp1, a late endosomal or lysosomal marker, although the association of Rab35 with the phagosomal membranes persisted even when Lamp1 appeared on

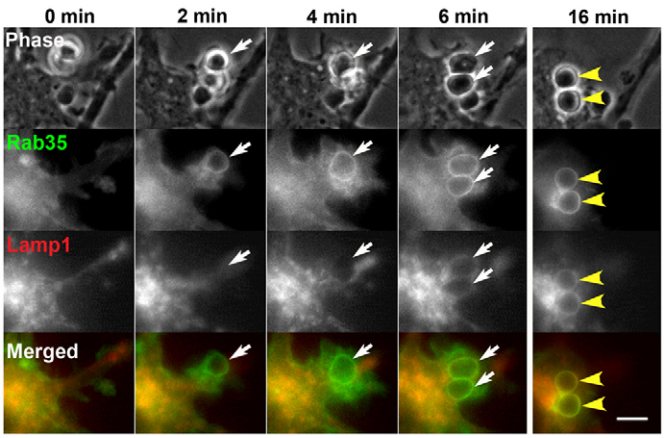

Fig. 1. Live-cell imaging of Rab35 and Lamp1 in RAW264 macrophages during the phagocytosis of IgG-Es. RAW264 cells co-transfected with GFP–Rab35 and CFP–Lamp1 were allowed contact with IgG-Es and observed by phase-contrast and fluorescence microscopy. Time-lapse images were recorded using the MetaMorph imaging system. Phase-contrast images are shown (top panels). Binding of IgG-Es to the cell surface is set as time 0. Note the localization of Rab35 at the early stage of phagosome formation (arrows). Rab35 is also found in Lamp1-positive phagosomes at around 16 minutes after IgG-E internalization (arrowheads). Representative images are shown. The corresponding video is supplementary material Movie 1. Scale bar: 5 μm.

them (Fig. 1 and supplementary material Movie 1). Thus, Rab35 was associated with the phagosomal membranes over an extended time period, from the early to the late stage of phagocytosis. These findings indicate that Rab35 functions not only in the process of maturation of phagosomes to phagolysosomes, but also in phagosome formation.

The increase in the fluorescence intensity of GFP–Rab35 in the phagocytic cups might be caused simply by an increase in membrane volume in the optical section and/or by the doubling of the membrane structures of the phagocytic cups. Therefore, to demonstrate the real changes in Rab35 concentration relative to the membrane volume of the phagocytic structures during phagocytosis, we applied the ratio imaging of GFP–Rab35 relative to CFP with a membrane-targeting signal (CFP–Mem), which uniformly labels the membrane, by a method described previously (Araki et al., 2007). As shown in Fig. 2A,B and supplementary material Movie 2, the ratio of GFP–Rab35 to CFP–Mem rapidly increased in the forming phagosomes and then gradually decreased after phagosome internalization. Quantitative analysis of the ratio images also indicated that the levels of Rab35 in the phagocytic membranes increased immediately after IgG-E binding, reaching a level more than three times that in non-phagocytic plasma membranes within about 1–2 minutes (Fig. 2C). Although the levels of Rab35 at the phagosomal membranes tended to decrease after 3–5 minutes, the levels of Rab35 in the membranes of phagosomes were maintained at higher than basal levels for an hour.

It is known that actin cytoskeleton remodeling during phagocytosis is tightly linked to phosphoinositide metabolism, which modulates the location and activity of actin-binding proteins (Yeung et al., 2006). For instance, the levels of PtdIns(4,5)P_2 increase in the membranes of extending pseudopodia driven by actin polymerization, but decrease in the base of phagocytic cups

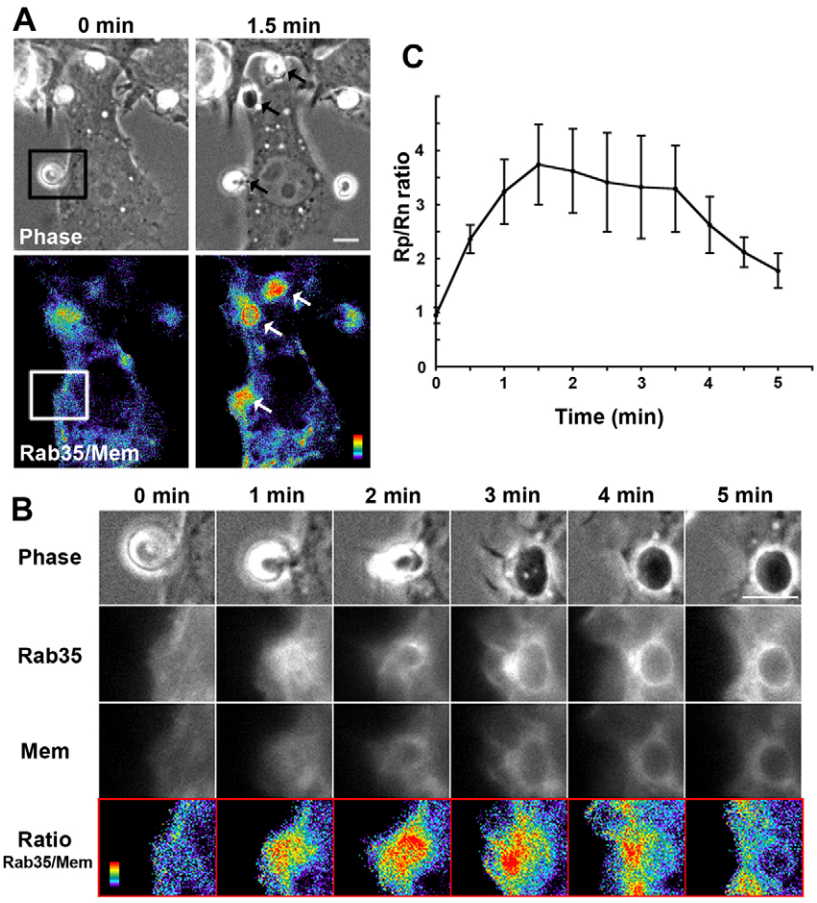

Fig. 2. Ratiometric image analysis demonstrating the changes in Rab35 concentration in the phagocytic membranes. (**A**) RAW264 cells were co-transfected with GFP–Rab35 and CFP–Mem. Time-lapse images of phase-contrast, GFP–Rab35 and CFP–Mem were taken by phase and fluorescence microscopy. The GFP/CFP ratio images showing the levels of Rab35 concentration in the membrane were obtained by digital image analysis using the MetaMorph imaging system. Arrows indicate increased levels of Rab35 at the sites of phagosome formation. The binding of IgG-Es to the cell surface, marked by squares, is set as time 0. The results were reproducible in independent experiments. Scale bar: 5 μm. (**B**) Selected images of the engulfed sites marked by squares in Fig. 2A. Scale bar: 5 μm. (**C**) Plots of the Rp/Rn ratio indicating the relative concentration of GFP–Rab35 in the phagocytic membrane. The Rp/Rn ratio was calculated by dividing GFP–Rab35/CFP–Mem ratio value in the phagocytic membrane (Rp) by that in the non-phagocytic membrane (Rn), to normalize the change in Rab35 levels in cells expressing variable amounts of GFP–Rab35 and CFP–Mem. The data are expressed as means (±s.e.m.) of five independent experiments.

where the actin filaments are dissociated from the membrane, when the phagocytic cups close into intracellular phagosomes (Botelho et al., 2000; Scott et al., 2005; Swanson and Hoppe, 2004). Meanwhile, PtdIns(3,4,5)P_3 is produced in the inner membrane of the phagocytic cups by PI3kinase, which is required for the completion of phagosome formation (Araki et al., 1996; Cox et al., 1999; Swanson, 2008; Vieira et al., 2001). To determine the structural and functional stages of phagocytosis with which Rab35 is associated, we coexpressed GFP–Rab35 and CFP–probes specific for PtdIns(4,5)P_2 or PtdIns(3,4,5)P_3 in RAW264 macrophages. First, we compared the localization of Rab35 and PtdIns(4,5)P_2 during FcγR-mediated phagocytosis in cells co-transfected with GFP–Rab35 and CFP–phospholipase Cδ1 (PLC)-pleckstrin homology domain (PH), which binds to PtdIns(4,5)P_2. Time-lapse imaging revealed that the Rab35 accumulation occurred at almost the same time as PtdIns(4,5)P_2 (Fig. 3A, supplementary material Movie 3), but their localization was not exactly the same in the forming phagosome. Although PtdIns(4,5)P_2 was richly produced in the outer wall of the phagocytic cups, Rab35 was predominantly localized in the base of the cups (Fig. 3A, supplementary material Fig. S1).

Next, we drew comparisons of the subcellular localization between Rab35 and PtdIns(3,4,5)P_3 during phagocytic cup formation. Time-lapse observations of live RAW264 macrophages coexpressing GFP–Rab35 and CFP–Akt-PH, which binds mainly to PtdIns(3,4,5)P_3, revealed that Rab35 and PtdIns(3,4,5)P_3 were largely colocalized at the phagocytic cups (Fig. 3B, supplementary material Movie 4). Remarkably, the fluorescence intensities of GFP–Rab35 and CFP–Akt-PH increased at the base of the phagocytic cups as the phagosomes closed (arrows in Fig. 3B). Subsequently, their intensities tended to decrease soon after the phagosome internalization. These findings indicate that Rab35, as well as PtdIns(3,4,5)P_3, is abundant at the inner membrane of the phagocytic cups (supplementary material Fig. S1).

Expression of Rab35 mutants and endogenous Rab35 knockdown inhibit FcγR-mediated phagocytosis

The localization of Rab35 at the early stages of phagocytosis in RAW264 cells strongly implies that Rab35 participates in phagosome formation. Hence, to confirm the functional contribution of Rab35 to FcγR-mediated phagosome formation, we examined the effects of the expression of Rab35 mutants and Rab35 silencing by RNAi on the binding of IgG-Es to the cell surface and on their internalization into phagosomes. We transiently transfected RAW264 macrophages with wild-type (wt) Rab35, GTP-bound mutant Rab35-Q67L (active form) or GDP-bound mutant Rab35-S22N (inactive form). Then, a quantitative assay of the binding and phagocytosis of IgG-Es was performed using cells expressing each Rab allele. As shown in Fig. 4, the expression of either GFP–Rab35-S22N or GFP–Rab35-Q67L led to the inhibition of the phagocytosis of IgG-Es, in contrast to nontransfected controls. However, the binding of IgG-Es to cells was not significantly affected by the expression of Rab35 wt, Rab35-Q67L or Rab35-S22N protein (Fig. 4).

Next, we adopted the RNAi approach to knock down endogenous Rab35 in RAW264 macrophages; cells were stably

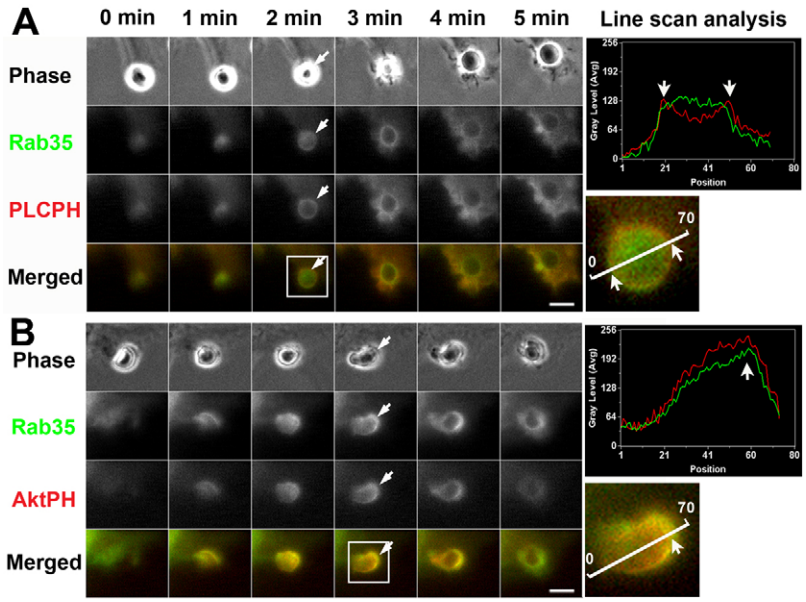

Fig. 3. Recruitment and localization of Rab35 with respect to phosphoinositides during phagosome formation. (**A**) Live RAW264 cells coexpressing GFP–Rab35 (green) and CFP–PLC-PH (red), which shows the localization of PtdIns(4,5)P_2, were incubated with IgG-Es and monitored by phase-contrast and fluorescence microscopy. Representative images of three independent experiments are shown. Scale bar: 5 μm. Rab35 recruitment to the membrane overlaps with the elevated levels of PtdIns(4,5)P_2 in time. Boxed area is enlarged in the bottom right panel. Line-scan analysis using the MetaMorph program shows fluorescence intensities of GFP–Rab35 (green) and CFP–PLC-PH (red) at the position of line in the enlarged image of boxed area. It is noteworthy that green fluorescence is predominant at the base of phagocytic cup, whereas red fluorescence is at the outer wall of phagocytic cup (arrows). (**B**) Time-lapse images of RAW264 macrophages coexpressing GFP–Rab35 (green) and CFP–Akt-PH (red), which shows the localization of PtdIns(3,4,5)P_3, were acquired in the same way as for Fig. 3A. Note the colocalization of Rab35 and PtdIns(3,4,5)P_3 at the base of the phagocytic cup (arrows). Line-scan analysis indicates that Rab35 and PtdIns(3,4,5)P_3 fluorescent intensities are correlative. The corresponding time-lapse videos of Fig. 3A and 3B are supplementary material Movies 3 and 4, respectively. Scale bar: 5 μm.

transfected with plasmids coding for several short hairpin RNAs (shRNAs). As shown in Fig. 5A, the stable expression of Rab35 shRNAs (GI562878, GI562879 and GI562881) significantly decreased Rab35 protein levels in RAW264 cells, whereas neither construct had any effect on Rab11 expression, as assessed by western blot analysis. Then, we performed the quantitative phagocytosis assay on these stable transformant cell lines. The efficiency of the phagocytosis and binding of IgG-Es in each Rab35 shRNA transfectant was compared with that in control cells stably transfected with empty shRNA vector. The depletion of endogenous Rab35 by RNAi led to the inhibition of phagocytosis to a degree comparable to that observed in cells expressing the GDP- or GTP-bound mutant of Rab35 (Fig. 5B). It is unlikely that the inhibition of phagocytosis by Rab35 shRNA expression was caused by a decrease in the binding of IgG-Es, because the binding of IgG-Es was not affected by the Rab35 knockdown (Fig. 5B). These results indicate that the binding of IgG-Es to FcγRs does not require functional Rab35, but that the internalization of IgG-Es into phagosomes does require normal cycling of Rab35 between GTP- and GDP-bound forms.

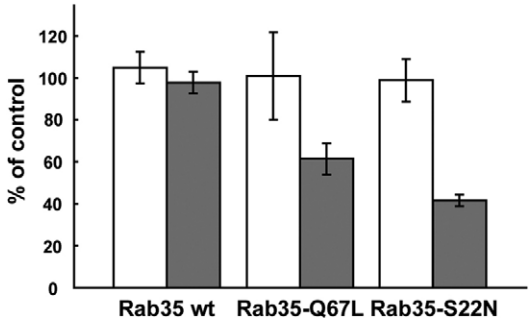

Fig. 4. Effect of active and inactive Rab35 mutant expression on FcγR-mediated phagocytosis and the binding of IgG-Es. To quantify phagocytosis, RAW264 cells transiently expressing GFP–Rab35 wt, GFP–Rab35-Q67L or GFP–Rab35-S22N were incubated with IgG-Es for 20 minutes at 37℃. The cells were fixed after disruption of the extracellularly exposed IgG-Es. The efficiency of phagocytosis was calculated based on 50 transfected and 50 untransfected cells. The results are expressed as a percentage of control (untransfected) cells (gray bars). The means ± s.e.m. of three independent experiments are plotted. For the binding assay, RAW264 cells transfected with each indicated construct were incubated with IgG-Es for 30 minutes at 4℃. After brief washing, the cells were fixed. The efficiency of IgG-E binding to the cells was calculated based on 50 transfected and 50 control cells (open bars). The data are expressed as the means ± s.e.m. of four independent experiments.

The expression of GDP-bound mutant Rab35-S22N decreases the surface area of macrophages undertaking frustrated phagocytosis

The observation of macrophages spreading on IgG-coated coverslips, in a process called ‘frustrated phagocytosis’ enables us to quantify the extent of pseudopod extension driven by actin cytoskeleton reorganization and/or membrane insertion from intracellular compartments (Cox et al., 1999). Hence, we used a frustrated phagocytosis assay to evaluate the effects of Rab35 expression on the increment of the surface area of macrophages on IgG-opsonized coverslips. Bone-marrow-derived macrophages expressing GFP–Rab35 wt, GFP–Rab35-Q67L or GFP–Rab35-S22N were plated on IgG-coated coverslips and fixed. After attachment to the IgG coverslips, the macrophages quickly spread along the IgG-coated surface and increased the area of attachment to engage in frustrated phagocytosis as previously described (Cannon and Swanson, 1992). It is noteworthy that the expression of GDP-bound mutant Rab35-S22N decreased the spreading area of macrophages on the IgG-coated coverslips ($P<0.05$), whereas neither the expression of Rab35 wt nor that of GTP-bound mutant Rab35-Q67L affected the spreading behavior (Fig. 6A,B). These data suggest that Rab35 is implicated in pseudopod extension by regulating the actin reorganization and/or exocytic insertion of membrane from intracellular reservoirs.

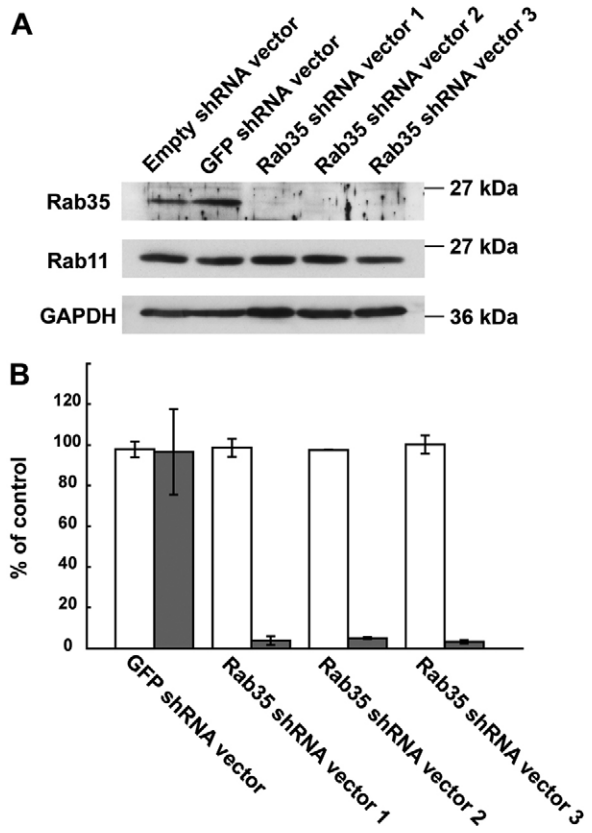

Fig. 5. Effect of Rab35 knockdown by shRNAs on FcγR-mediated phagocytosis and the binding of IgG-Es. (**A**) RAW264 cells stably transfected with each construct indicated were subjected to detergent lysis, SDS-PAGE, and immunoblotting with anti-Rab35, anti-Rab11 or anti-GAPDH antibody. Rab11 and GAPDH were used as internal controls. (**B**) The efficiency of IgG-E phagocytosis (gray bars) and IgG-E binding (open bars) calculated based on 50 cells expressing each Rab35 shRNA and 50 control cells stably transfected with GFP shRNA or empty shRNA vector. The results are expressed as a percentage of control cells transfected with empty shRNA plasmid. The means ± s.e.m. of three independent experiments are plotted.

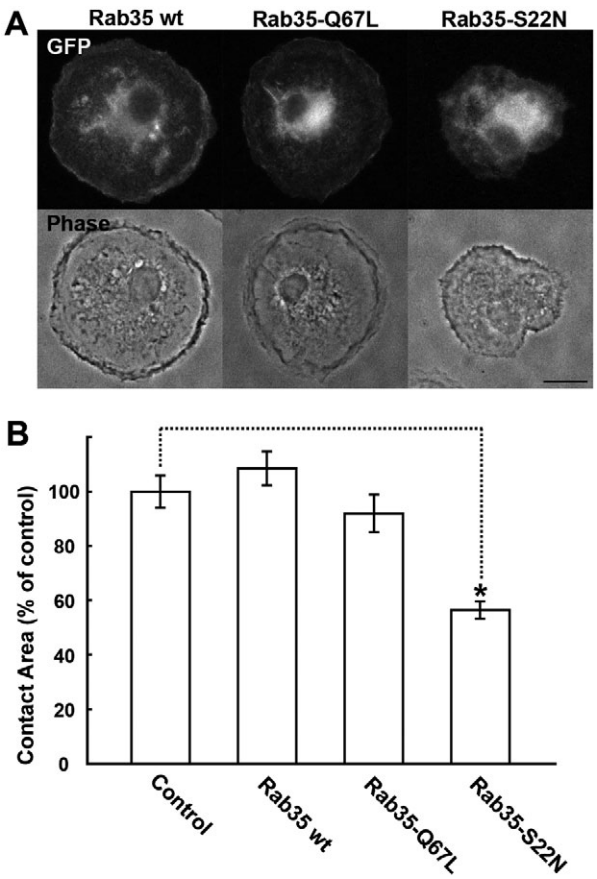

Fig. 6. Quantitative assay of pseudopod extension along the IgG-coated surface by frustrated phagocytosis model. (**A**) Bone marrow-derived macrophages expressing GFP–Rab35 wt, GFP–Rab35-Q67L or GFP–Rab35-S22N were seeded onto IgG-coated coverslips, incubated at 37℃ for 20 minutes and fixed. The effects of each Rab35 mutant on cell spreading were examined by phase-contrast and fluorescence microscopy. Representative images are shown. Scale bar: 10 μm. (**B**) Quantification of the extent of pseudopod extension by measuring the cell spreading area on IgG-coated coverslips using the MetaMorph imaging system. The spreading areas of 50 cells/coverslip were measured. The values expressed as a percentage of control (untransfected) cells are means ± s.e.m. of three independent experiments. Student's *t*-test was used for statistical analysis. *$P<0.05$.

Rab35 is involved in actin cytoskeleton remodeling but not actin assembly during FcγR-mediated phagocytosis

It is well known that the dynamic assembly and remodeling of the actin cytoskeleton during FcγR-medicated phagocytosis is coordinated by Rho-family GTPases and phosphoinositides (Swanson, 2008). Recently, it has been reported that Rab35 might also participate in the regulation of actin remodeling during neurite outgrowth and *Drosophila* bristle development (Chevallier et al., 2009; Zhang et al., 2009). These studies indicate that Rab35 might also be involved in actin assembly and/or remodeling during phagosome formation. We first examined the effect of the expression of Rab35-S22N (GDP-bound mutant) on the assembly of F-actin at the sites of phagocytosis in RAW264 macrophages 5 minutes after the addition of IgG-Es. After F-actin staining with Rhodamine–phalloidin, the percentage of F-actin assembly at IgG-E binding sites was scored under a microscope. We found that F-actin assembly was present in 73.7±9.8% of sites of IgG-E binding in Rab35-S22N-expressing cells and 70.6±12% of those in non-expressing controls, suggesting that the initial assembly of F-actin at IgG-E binding sites was not significantly affected by the expression of Rab35-S22N.

We next examined the spatiotemporal relationship between Rab35 and actin dynamics in live RAW264 macrophages coexpressing GFP–actin and TagRFP-Rab35 during the phagocytosis of IgG-Es. Time-lapse image analysis showed that both proteins were closely localized around forming phagosomes (Fig. 7A, supplementary material Movie 5). It is notable that Rab35 is more abundant at the base of the phagocytic cups where actin disassembly and remodeling actively occur rather than at the extending edge of phagocytic cups (Fig. 7A, supplementary material Movie 6 and Fig. S1). To confirm the functional role of Rab35 in actin remodeling, we co-transfected RAW264 cells with GFP–actin and TagRFP-Rab35-S22N (GDP-bound inactive form) and analyzed the actin dynamics during IgG-E uptake. Before the addition of IgG-Es to the macrophages, TagRFP-Rab35-S22N was less closely associated with the plasma membrane and homogeneously localized in the cytosol, as previously reported for other cell types (Zhang et al., 2009). Even after the binding of IgG-Es to the cell surface, we did not

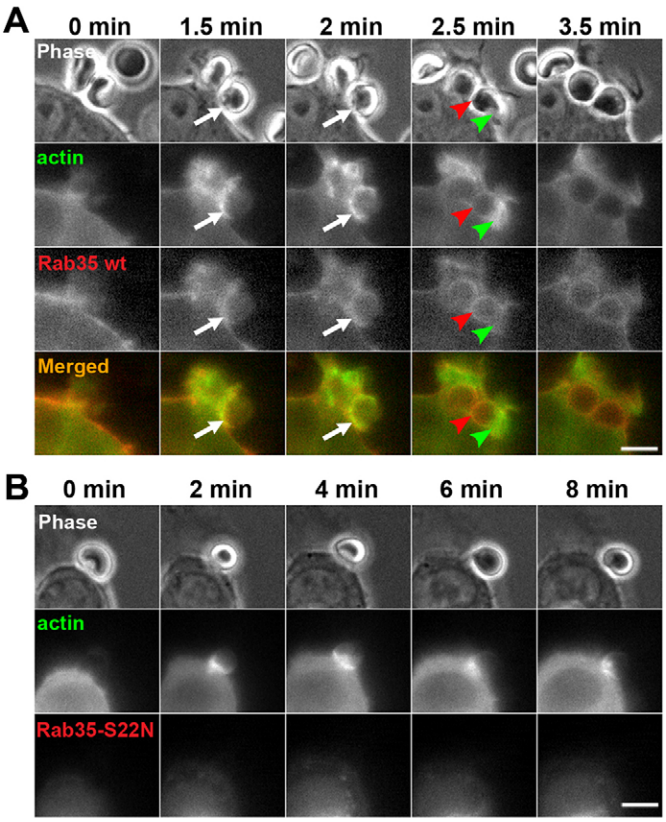

Fig. 7. Time-lapse imaging showing the spatiotemporal relationship between Rab35 and actin during phagosome formation. (**A**) Live RAW264 cells coexpressing GFP–actin and TagRFP–Rab35 wt were put into contact with IgG-Es and observed by phase-contrast and fluorescence microscopy. A side view of phagosome formation shows that Rab35 recruitment and F-actin assembly occurs concomitantly during pseudopod extension (arrows). As the phagocytic cup closes, Rab35 is predominantly localized at the base of the phagocytic cup (red arrowheads), whereas actin is enriched at the leading edge of the closing cup (green arrowheads). Scale bar: 5 μm. The corresponding video is supplementary material Movie 6. (**B**) Time-lapse images of RAW264 cells coexpressing GFP–actin (green) and TagRFP–Rab35-S22N (red) recorded in the same way as in A. Although inactive Rab35 is not recruited to the membrane, actin assembly is seen at the site of IgG-E binding. Strikingly, subsequent phagocytic cup formation is inhibited in the cells. Scale bar: 5 μm.

observe any changes in the localization of TagRFP-Rab35-S22N, indicating that the GDP-bound mutant of Rab35 is not recruited to the phagosomal membranes (Fig. 7B). Live-cell imaging also showed that actin assembly occurred at the IgG-E binding sites in the cells expressing Rab35-S22N, whereas the pseudopod extension was insufficient to form full-grown phagocytic cups (Fig. 7B, supplementary material Movie 7). Only short protrusions of the plasma membrane were formed around the binding IgG-Es, but they diminished without extending to form full-grown phagocytic cups (supplementary material Movie 7). Notably, in the cells expressing inactive Rab35, a dense actin coat was retained for a while underneath the membrane of IgG-E binding sites (Fig. 7B), whereas actin distribution became sparse at the base of the phagocytic cups in the control cells. Similar results were obtained in Rab35-depleted stable cell lines established by RNAi (data not shown). These characteristics described above were not found in control macrophages expressing GFP–actin or coexpressing GFP–actin and TagRFP-Rab35 wt (Fig. 7A, supplementary material Movie 6).

To further define the effect of Rab35 knockdown on phagosome formation, RAW264 cells stably transfected with GFP shRNA (control) or Rab35 shRNA were observed by scanning electron microscopy (EM). In control macrophages expressing GFP shRNA, after 10 minutes of incubation with IgG-Es, some IgG-Es were seen on the dorsal surface and others were internalized in the cell body (Fig. 8A). Under this condition, phagocytic cups at various stages of development were observed at higher magnification. It is notable that the phagocytic cups developed well along the surface of the IgG-Es, frequently showing cylindrical structures containing IgG-Es (Fig. 8B). In Rab35-knockdown macrophages generated by RNAi, more IgG-Es were found on the dorsal cell surface (Fig. 8C). At high magnification of the Rab35-knockdown cells, however, pseudopod extension to form phagocytic cups appeared to be

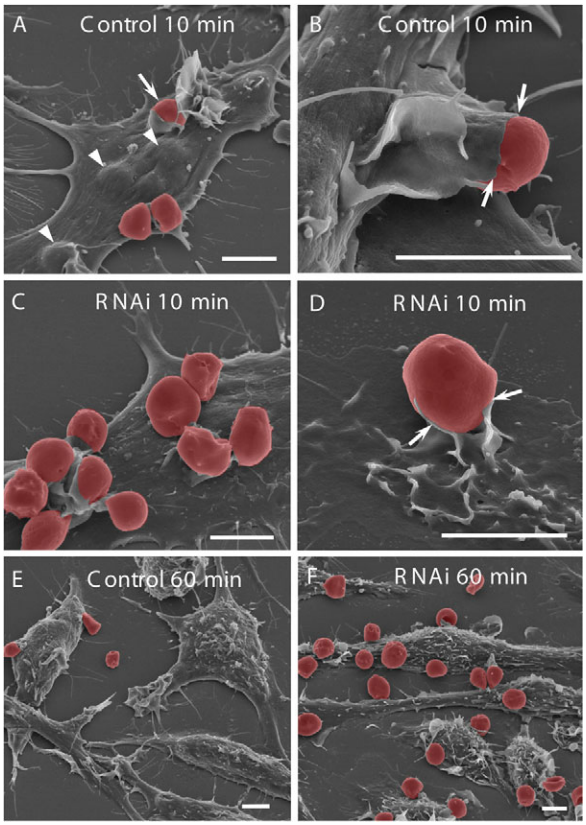

Fig. 8. Scanning EM observation of FcγR-mediated phagocytosis of IgG-Es in control and Rab35-knockdown RAW264 macrophages. RAW264 cells expressing control GFP shRNA (**A**,**B**,**E**) or Rab35 shRNA (**C**,**D**,**F**) were incubated with IgG-Es for 10 minutes (A–D) or 60 minutes (E,F) at 37℃, then fixed and processed for scanning EM. In the control macrophages 10 minutes after the addition of IgG-Es (A,B), some IgG-Es were seen on the dorsal surface of the cells (arrows), and others were already internalized into the cells (arrowheads). Note the pseudopod extension along the surface of the IgG-Es (arrows in B). In Rab35-knockdown cells (C,D), pseudopod extension is severely impaired (arrows in D), whereas many IgG-Es are bound to the dorsal cell surface (C). After 60 minutes, almost all IgG-Es are internalized in the control cells (E), whereas many IgG-Es still remain on the cell surface of Rab35-knockdown cells (F). IgG-Es are pseudocolored by Adobe Photoshop CS3. Scale bars: 5 μm.

severely impaired, whereas cell surface ruffles were sometimes seen. We found only shallow cups or pedestal-like structures under the IgG-Es (Fig. 8D). Sixty minutes after the addition of the IgG-Es, few IgG-Es were seen on the dorsal surface of the control macrophages, because almost all of the IgG-Es had been internalized into the cell body (Fig. 8E). However, many IgG-Es were still observed on the dorsal surface of the Rab35-knochdown cells by Rab35 RNAi (Fig. 8F), suggesting that phagocytic cup formation and IgG-E internalization were greatly inhibited.

ACAP2 functions as a downstream effector of Rab35 during phagosome formation

Most recently, it has been reported that ACAP2, a GAP (GTPase activating protein) for ARF6, binds Rab35 and controls Rab35-dependent neurite outgrowth of PC12 cells through inactivation of ARF6 (Kanno et al., 2010). ACAP2 has been shown to be ubiquitously expressed (Jackson et al., 2000) and was also detected in RAW264 macrophages by western blotting and RT-PCR analysis (supplementary material Fig. S2). Therefore, we investigated the possible role of ACAP2 as a Rab35 downstream effector in controlling phagosome formation. First, we observed the subcellular localization of ACAP2 during FcγR-mediated phagocytosis in macrophages. Time-lapse observation of live RAW264 cells expressing GFP–ACAP2 indicated that before the onset of phagocytosis ACAP2 was distributed throughout the cytosol, as previously shown in other cell types (Jackson et al., 2000; Kanno et al., 2010). After the binding of IgG-E to the cell surface, ACAP2 was recruited to the membrane of the phagocytic cup (Fig. 9A). Subsequently, ACAP2 was temporally localized on the membrane of newly formed phagosomes and then dissociated over time.

It is known that the GTP-bound form of Rab35 directly interacts with ankyrin repeat domain (ANKR) of ACAP2 in vitro (Kanno et al., 2010). To determine whether Rab35 recruits ACAP2 to the phagocytic membrane in a GTP-dependent manner, we examined the effect of expression of Rab35-Q67L or Rab35-S22N on the recruitment of ACAP2 to the phagocytic cup in RAW264 macrophages. Expression of Rab35-Q67L promoted the relocalization of ACAP2 to the plasma membrane in agreement with the previous study using other cell lines (Kanno et al., 2010). Note that the recruitment of ACAP2 to sites of phagocytic cup formation was markedly enhanced by coexpression with Rab35-Q67L (Fig. 9B). Curiously, coexpression of ACAP2 with Rab35-Q67L maintained the association of ACAP2 with the membrane of phagocytic cups, and impaired the closure of phagocytic cups (supplementary material Movie 8). This implies that temporal association of Rab35 followed by disassociation from the membrane is required for the completion of phagosome formation.

Coexpression of ACAP2 with Rab35-S22N did not induce the recruitment of ACAP2 to sites of IgG-E-binding (Fig. 9C), suggesting that the recruitment of ACAP2 to sites of phagosome formation is dependent on GTP-bound Rab35. In a quantitative assay of phagocytosis (Fig.10), the expression of GFP–ACAP2 alone reduced the efficiency of phagocytosis slightly, but significantly ($P<0.05$). The expression of Rab35 binding-defective mutant of ACAP2 (ACAP2-ΔANKR) or ARF6-GAP defective mutant of ACAP2 (ACAP2-RQ) had less effect on phagocytosis of IgG-Es. Intriguingly, the efficiency of phagocytosis in cells coexpressing ACAP2 and Rab35-Q67L was significantly lower than that in cells expressing Rab35-Q67L alone, indicating that the coexpression of ACAP2 with Rab35-Q67L results in a synergistic decrease in the ingestion of IgG-Es. However, coexpression of ACAP2-ΔANKR or ACAP2-RQ with Rab35-Q67L did not show such synergistic inhibitory effect on the rate of phagocytosis. In contrast to the effect on the ingestion of IgG-Es, the binding of IgG-Es to cells was not affected by the coexpression of ACAP2 with Rab35-Q67L (Fig. 10).

To clarify the functional link between Rab35 and ARF6, we examined the involvement of GTP-bound Rab35 in the regulation of ARF6 activity during FcγR-mediated phagocytosis. We generated RAW264 stable cell lines expressing GFP–Rab35-Q67L, and then monitored the activation levels of endogenous ARF6. The activation of ARF6 was severely inhibited in cells expressing GTP-bound mutant of Rab35 compared with those expressing GFP control (supplementary material Fig. S3A). Moreover, no activation of ARF6 was detected in macrophages expressing GFP–Rab35-Q67L during FcγR-mediated phagocytosis (supplementary material Fig. S3B).

Discussion

Our study provides the first evidence that Rab35 is actively recruited to the phagocytic membrane where IgG-opsonized particles bind and that it participates in the regulation of FcγR-medicated phagosome formation through recruitment of ACAP2, even though Rab35 is implicated in the fusion of phagosomes and lysosomes during the process of phagosome maturation (Smith et al., 2007). At the initial stage of phagosome formation, signal transduction from IgG-ligated FcγR induces production of PtdIns(4,5)P_2, leading to actin polymerization and assembly beneath the plasma membrane at the binding sites of IgG-opsonized particles (Botelho et al., 2000). These events are believed to contribute to the formation of membrane protrusions that surround the phagocytic targets. Activation of Rho-GTPases such as Cdc42 and Rac1 is also required for the actin reorganization in the leading edge of phagocytic cups and pseudopodia (Cox et al., 1997; Hoppe and Swanson, 2004; Massol et al., 1998). Moreover, the conversion of PtdIns(4,5)P_2 to PtdIns(3,4,5)P_3 by PI3-kinase is crucial for further actin remodeling and/or membrane trafficking, to form full-grown phagocytic cups and to close phagosomes (Araki et al., 1996; Cox et al., 1999; Marshall et al., 2001). Thus, the processes of phagosome formation are dependent on complex events of membrane trafficking and actin cytoskeleton reorganization, which are spatiotemporally coordinated by many regulatory molecules. In this study, we revealed that Rab35 is recruited to the membranes of phagocytic cups where PtdIns(4,5)P_2 is enriched, after which Rab35 accumulates at the base of the phagocytic cups in a way similar to PtdIns(3,4,5)P_3. Although the functional link between Rab35 and these phosphoinositides is unclear, it may be possible that the recruitment and localization of Rab35 to the phagocytic membranes are related to the levels of the phosphoinositides, since the C-terminal of Rab35 has unique polybasic clusters that bind to PtdIns(4,5)P_2 and PtdIns(3,4,5)P_3 (Heo et al., 2006).

Our time-lapse microscopy of live cells and scanning EM analysis suggest that the expression of GDP-bound mutant Rab35-S22N or the depletion of endogenous Rab35 by RNAi results in the impairment of pseudopod extension to form phagocytic cups. Moreover, in a model of frustrated phagocytosis, the expression of the GDP-bound mutant of

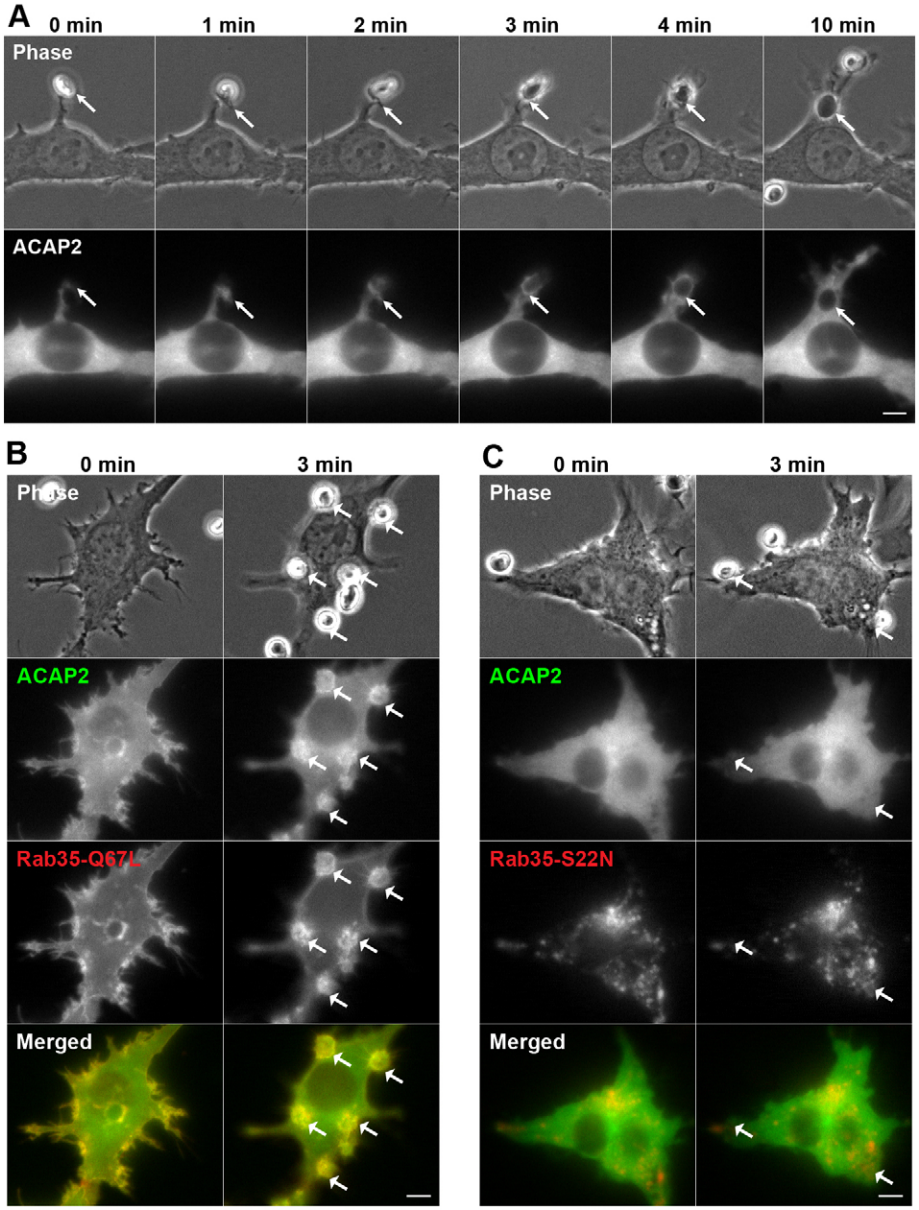

Fig. 9. Recruitment and localization of ACAP2 during FcγR-mediated phagocytosis. (**A**) Live RAW264 cells expressing GFP–ACAP2 were put into contact with IgG-Es (arrows) and observed by phase-contrast and fluorescence microscopy. Phase-contrast images are shown (top panels). Scale bar: 5 µm. (**B**) Time-lapse images of RAW264 cells coexpressing GFP–ACAP2 (green) and TagRFP-Rab35-Q67L (red) acquired using the MetaMorph imaging system. Representative images from four experiments are shown. Note the colocalization of ACAP2 and Rab35-Q67L at the phagocytic cups (arrows). Scale bar: 5 µm. (**C**) RAW264 cells co-transfected with GFP–ACAP2 (green) and TagRFP-Rab35-S22N (red) were observed in the same way as in B. It is noteworthy that both ACAP2 and Rab35-S22N are not recruited to the site of IgG-Es binding (arrows). Scale bar: 5 µm.

Rab35 significantly diminished the extent of pseudopod extension along the surface of the IgG-coated coverslips. These data all support the notion that activated Rab35 is crucial for pseudopod extension during FcγR-medicated phagocytosis. Interestingly, we found that the expression of GTP-locked mutant Rab35-Q67L also inhibited FcγR-medicated phagosome formation, whereas the expression of this mutant had a smaller effect on the extent of pseudopod extension along the surface of IgG-coated coverslips or IgG-Es. These results indicate that the activation of Rab35 is needed to form phagocytic cups, but it is not enough to complete phagosome formation. It is postulated that deactivation of Rab35 might also be required for a later step of phagosome formation, possibly cup closure.

It is of interest to know the downstream effectors and how Rab35 mechanistically controls phagosome formation. The local assembly and reorganization of an actin cytoskeleton during phagocytic cup formation is mediated by the recruitment and activation of actin-regulatory proteins such as Arp2/3 (May et al., 2000). Cdc42, a member of the Rho GTPase family, binds and activates WASP, which induces actin polymerization by activation of the Arp2/3 complex. During FcγR-medicated phagocytosis, the activation and deactivation of Cdc42 are required for phagocytic cup formation and cup closure, respectively (Beemiller et al., 2010). Recently, Rab35 has been shown to activate Cdc42 to regulate neurite outgrowth in PC12 and N1E cells, indicating that Rab35 has a role in modulating the actin cytoskeleton through Cdc42 activation (Chevallier et al., 2009). In addition, it has been reported that Rab35 mediates Cdc42 transport to the plasma membrane during scavenger receptor C1-mediated phagocytosis of *Candida albicans* in *Drosophila* SL2 cells (Shim et al., 2010). Therefore, it is possible that Rab35 regulates the recruitment and activation of Cdc42, which is required for actin remodeling, leading to phagocytic cup formation in macrophages. However, the

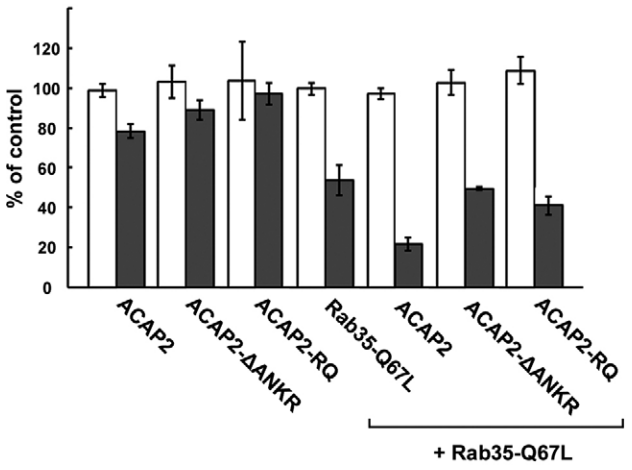

Fig. 10. Effect of ACAP2 expression on FcγR-mediated phagocytosis and the binding of IgG-Es. RAW264 cells expressing ACAP2 constructs and/or Rab35-Q67L were incubated with IgG-Es at 37℃ for 20 minutes. The efficiency of phagocytosis was calculated based on 50 transfected and 50 untransfected cells. The results are expressed as a percentage of control (untransfected) cells (grey bars). Data shown are the mean ± s.e.m. of three independent experiments. The efficiency of IgG-Es binding was calculated as described in the Materials and Methods. The results are expressed as a percentage of control (untransfected) cells (open bars). The data are expressed as the mean ± s.e.m. of three independent experiments.

molecular mechanism linking Rab35 to Cdc42 has not been established in macrophages.

In addition to Rho family GTPases, ARF6, an isoform of ARF family GTPases, has been shown to be engaged in the regulation of actin remodeling and membrane traffic in FcγR-medicated phagocytosis (Niedergang et al., 2003; Zhang et al., 1998). Zhang and colleagues reported that expression of an ARF6 mutant (GDP- or GTP-locked allele) inhibits FcγR-medicated phagocytosis, indicating that the inactivation-activation cycle of ARF6 is required for the proper remodeling of plasma membrane structure and actin-based cytoskeletal organization (Zhang et al., 1998). Importantly, in this study, it was found that ACAP2, a GAP for ARF6, accumulates in the membrane of phagocytic cups in a GTP-Rab35-dependent manner. The quantitative assay of phagocytosis revealed that coexpression of ACAP2 with GTP-locked Rab35 results in a remarkable synergistic decrease in the rate of IgG-Es ingestion, whereas the expression of the Rab35 binding-defective mutant (ACAP2-ΔANKR) or the ARF6-GAP defective mutant (ACAP2-RQ) caused no such synergistic impact on the efficiency of phagocytosis even if the GTP-bound Rab35 mutant was coexpressed. Therefore, it is likely that GTP-Rab35-dependent membrane targeting of ACAP2 through its ANKR domain and ARF6-GAP activity of ACAP2 might be needed to exert its function during phagosome formation.

The phagocytosis of large particles requires the addition of membrane from intracellular reservoirs. The focal delivery of these endomembranes to sites of phagocytosis, a process called 'focal exocytosis', is considered to facilitate the elongation of pseudopodia (Braun et al., 2004; Zhang et al., 1998). Because the expression of inactive ARF6 mutant inhibits the focal exocytosis of VAMP3-containing vesicles during FcγR-mediated phagocytosis (Niedergang et al., 2003), Rab35 might also be implicated in focal exocytosis as an upstream regulator of ARF6. However, it is unclear whether AFR6 directly regulates vesicle transport and/or fusion to the plasma membrane in focal exocytosis. It is also conceivable that inhibition of actin disassembly at the base of phagocytic cups results in blocking focal exocytosis because expression of GDP-bound mutant of Rab35 persistently retained a dense actin layer at the base of stalled phagocytic cups. In our preliminary observation, VAMP3-positive vesicles were found around the IgG-Es in cells expressing Rab35-S22N, indicating that the expression of Rab35-S22N has little effect on the vesicle transport for focal exocytosis. However, it was unclear by light microscopy whether blockade of vesicle fusion to the membrane of phagocytic cups normally occurs. Electron microscopic observations are required to resolve this issue in future studies.

Although Rab35 might have multiple downstream effectors involved in distinct steps of phagosome formation and maturation, this study emphasizes the important role of Rab35 in the regulation of phagosome formation by recruiting ACAP2, which can modulate ARF6 activity. Overall, it can be concluded that the temporal GDP–GTP cycle of Rab35 eventually regulates actin cytoskeleton and/or membrane delivery for pseudopod extension and phagocytic cup closure under the control of ARF6.

Materials and Methods

Reagents

Bovine serum albumin (BSA) and Dulbecco's modified Eagle's medium (DMEM) were obtained from Sigma (St Louis, MO). Fetal bovine serum (FBS) was obtained from BioSolutions International (Melbourne, Australia). Purified polyclonal anti-Rab35 antibody (Proteintech Group, Chicago, IL), monoclonal anti-Rab11 antibody (BD Transduction Laboratories, Palo Alto, CA) and anti-glyceraldehyde-3-phosphate dehydrogenase (GAPDH) antibody (Ambion, Huntington, UK) were purchased from commercial sources. The other reagents were purchased from Wako Pure Chemicals (Osaka, Japan) or Nakalai tesque (Kyoto, Japan), unless otherwise indicated.

Cell culture

Mouse macrophage RAW264 cells were cultured in DMEM supplemented with 10% heat-inactivated fetal bovine serum (FBS), 100 U/ml penicillin and 100 μg/ml streptomycin, as described in the manuals of the cell line bank. Before the experiments, the culture medium was replaced with Ringer's buffer (RB) consisting of 155 mM NaCl, 5 mM KCl, 1 mM $MgCl_2$, 2 mM Na_2HPO_4, 10 mM glucose, 10 mM HEPES, pH 7.2 and 0.5 mg/ml BSA.

Bone-marrow-derived macrophages were obtained from the femurs of C57BL/6 mice, as previously described (Araki et al., 2000). The cells were cultured for 6–8 days in the presence of macrophage-colony stimulating factor (M-CSF), and were used for frustrated phagocytosis assay.

DNA constructs and transfection

The full-length cDNA coding region of human *RAB35* was amplified by PCR. The fragment was cloned into the *Xho*I and *Bam*HI restriction sites of the pEGFP-C1 vector (Clontech, Palo Alto, CA). pEGFP-Rab35-S22N (GDP-bound mutant) and pEGFP-Rab35-Q67L (GTP-bound mutant) were generated by means of the QuikChange II site-directed mutagenesis kit (Stratagene, La Jolla, CA). pTagRFP-Rab35, pTagRFP-Rab35-S22N and pTagRFP-Rab35-Q67L were generated by the replacement of GFP with TagRFP. pEGFP-Actin and pECFP-Mem were purchased from Clontech (Palo Alto, CA). pEYFP-Lamp1, pECFP-phospholipase Cδ1 (PLC) pleckstrin homology domain (PH) and pECFP-Akt-PH were provided by Joel A. Swanson (University of Michigan, Ann Arbor, MI). pECFP-Lamp1 was generated by replacing yellow fluorescent protein (YFP) in pEYFP-Lamp1 with cyan fluorescent protein (CFP). pEGFP-ACAP2, pEGFP-ACAP2-ΔANKR and pEGFP-ACAP2-RQ were described previously (Kanno et al., 2010). All constructs were verified by sequencing. The RAW264 cells were transfected by electroporation. The cells were suspended at a concentration of 5×10^6 cells/ml in the growth medium. 400 μl of the cell suspension were mixed with 10 μg of plasmid DNA in a 4-mm-gap electroporation cuvette. Electroporation was performed using the ECM 630 Electroporation System (BTX Harvard Apparatus, MA) at 300 V, 1000 μf and 25 Ω, to yield a time constant of ~12 mseconds. The cells were then seeded onto 25 mm coverslips and maintained in the growth medium. Bone-marrow-derived macrophages were transfected using the Amaxa Nucleofector system kit for mouse macrophages (Amaxa GmbH, Cologne, Germany) according to the manufacturer's instructions. Briefly, 1×10^6

cells were transfected with 2 μg of plasmid DNA and cultured in growth medium. Experiments were performed 24–48 hours after transfection.

Silencing of endogenous Rab35 by shRNA

Short hairpin RNAs (shRNAs) were used to stably knock down Rab35 expression in RAW264 cells. Rab35 shRNAs that are cloned into pEGFP-V-RS vector were purchased from Origene (Rockville, MD). Three different Rab35 shRNAs (GI562878, GI562879 and GI562881) and a control shRNA (TR30007, negative control shRNA pGFP-V-RS plasmid; TR30008, negative control shRNA pGFP-V-RS non-effective tGFP plasmid) were used for transfection. The transfectants were selected with 5 μg/ml puromycin for 3 weeks to generate stable cell lines and were tested for the expression of Rab35 by western blot analysis.

Western blotting

Cells were washed with ice-cold phosphate-buffer saline (PBS) and suspended in lysis buffer containing 50 mM Tris-HCl (pH 7.5), 150 mM NaCl, 1% Triton X-100, 0.5% sodium deoxycholate, 0.1% sodium dodecyl sulfate (SDS), 0.1% CHAPS and protease inhibitor cocktail (Nacalai Tesque, Kyoto, Japan). The cell lysates were briefly sonicated at 4℃ and separated from the pellets after centrifugation at 12,000 r.p.m. for 15 minutes. Protein concentrations were estimated with the BCA protein assay reagent, and equal amounts of protein were denatured and reduced with a sample buffer containing 1% SDS and 2.5% 2-mercaptoethanol. Western blotting was carried out using a polyvinylidene difluoride (PVDF) membrane (Bio-Rad, Richmond, CA) and the ECL Plus Western Blotting detection system (GE Healthcare, Piscataway, NJ). The samples were subjected to SDS-PAGE and transferred to the PVDF membrane. The membrane was blocked with 5% nonfat dry milk in PBS containing 0.1% Tween 20 for 30 minutes at room temperature and probed with primary antibody at 4℃ overnight. After washing, the membrane was incubated with horseradish peroxidase conjugated with anti-rabbit or anti-mouse secondary antibody (dilution 1:10,000) for 2 hours at room temperature, developed using an ECL Plus regent and exposed to Hyperfilm (GE Healthcare, Piscataway, NJ). The following primary antibodies were used: anti-Rab35 antibody (1:1000), anti-Rab11 antibody (1:2000) and anti-GAPDH antibody (1:10,000).

Phagocytosis assay

Sheep erythrocytes were opsonized with rabbit anti-sheep erythrocyte IgG (1:200, Organo Teknika-Cappel) and resuspended in PBS as described previously (Araki et al., 1996). For the quantitative assay of phagocytosis, IgG-opsonized erythrocytes (IgG-Es) were added to adherent RAW264 macrophages. After 20 minutes of incubation with IgG-Es at 37℃, the cells on the coverslips were dipped into distilled water for 2 minutes to disrupt the extracellularly exposed IgG-Es, and were fixed with 4% paraformaldehyde and 0.1% glutaraldehyde. The number of internalized IgG-Es was counted in 50 cells randomly chosen under a phase-contrast and fluorescence microscope. The phagocytic index, i.e. the mean number of IgG-Es taken up per cell, was calculated. The index obtained for the transfected cells was divided by the index obtained for the nontransfected (control) cells and expressed as a percentage of the control cells. For the binding assay, RAW264 cells were incubated with IgG-Es for 30 minutes at 4℃, briefly washed in ice-cold PBS to remove the unbound IgG-Es and fixed. We then counted the number of cell-bound IgG-Es, and calculated the binding index, i.e. the mean number of bound IgG-Es per cell. The binding index was expressed as a percentage of the control nontransfected cells.

Frustrated phagocytosis assay

Frustrated phagocytosis assay was conducted according to a modified procedure based on a previous report (Cannon and Swanson, 1992). Transfected bone-marrow-derived macrophages were suspended in RB and then added to human IgG-coated coverslips containing RB. 20 minutes after the cells were plated on the coverslips at 37℃, the cells were washed and fixed with 4% paraformaldehyde. The spreading area of 50 cells in close contact with the IgG-coated coverslips was measured by the MetaMorph imaging system. Experiments were performed in triplicate. The cell spreading index represents the percentage of nontransfected (control) cells.

Live-cell microscopy and image analysis

RAW264 cells were cultured onto 25 mm circular coverslips and assembled in an RB-filled chamber on the thermo-controlled stage (Tokai Hit INU-ONI, Shizuoka, Japan) of an inverted epifluorescence microscope (Nikon TE300, 100× NA 1.35 oil-immersion objective). We used the wide-filed microscopy with a broad focal plane rather than confocal laser microscopy, to follow the steps of phagosome formation from the cell surface.

Phase-contrast and fluorescence images of live cells were sequentially taken through a cooled CCD camera (Retiga Exi, QImaging, Surrey, BC, Canada) using the MetaMorph imaging system (Molecular Devices Downingtown, PA). In the cells coexpressing GFP and CFP fusion proteins, GFP and CFP images were acquired using a YFP filter set of excitation 505 nm and emission 540 nm and a CFP set of excitation 435 nm and emission 490 nm, respectively, to separate one signal from another. We could confirm that neither fluorescence signal was detected through the other filter set. Time-lapse images of phase-contrast and fluorescence microscopy were taken at 10 second intervals and assembled into QuickTime movies by means of the MetaMorph imaging system, as previously described (Araki et al., 2007). Line-scan analysis was performed using the MetaMorph software.

Ratiometric imaging was used to monitor the changes in Rab35 levels in the plasma membrane during phagocytosis. Fluorescent images of GFP–Rab35 and CFP–Mem, which uniformly labels plasma membrane and phagosomal membrane, were sequentially acquired. After background subtraction, ratio images of GFP–Rab35/CFP–Mem were created using the MetaMorph software. The ratio images reported the concentrations of GFP-fusion proteins relative to the membrane, thereby correcting for variations in optical path length relative to cell shape or membrane volume (Araki et al., 2007). For quantitative image analysis of Rab35 levels during particle uptake, we defined time 0 as the moment when IgG-E binds to the cell surface to synchronize the data from several phagocytic events occurring in the cell. Then, we measured the ratio values of GFP–Rab35/CFP–Mem in the regions of interest, which were manually selected every 30 seconds throughout the time course after particle attachment. The ratio values of GFP–Rab35/CFP–Mem in the phagocytic membrane (Rp) were further divided by the average value of GFP–Rab35/CFP–Mem ratio in the non-phagocytic plasma membrane (Rn), to provide a normalized ratio (Rp/Rn) for different expression levels of both fluorescent proteins. Dividing Rp by Rn reported the relative concentration of GFP fusion proteins on the phagosomal membrane in cells expressing variable amounts of GFP–Rab35 and CFP–Mem (Araki et al., 2007; Hoppe and Swanson, 2004).

Scanning EM

RAW264 cells were cultured on plastic sheets and incubated with IgG-Es at 37℃. The cells were fixed with 2% glutaraldehyde in 0.1 M phosphate buffer, pH 7.4, containing 5% sucrose for 1 hour at room temperature. The cells on plastic sheets were rinsed in a buffer, post-fixed with 1% osmium tetroxide, treated with 1% tannic acid and 1% osmium tetroxide, and conventionally processed for scanning EM. Critical-point-dried specimens were coated with an osmium plasma coater and observed by a field emission scanning electron microscope (Hitachi S900), as previously described (Araki et al., 1996).

Acknowledgments

The authors would like to thank Joel A. Swanson for providing pEYFP-Lamp1, pECFP-PLC-PH and pECFP-Akt-PH plasmids. We also thank Katsuya Miyake and Makoto Fujii for their helpful discussion, and Kazuhiro Yokoi, Yukiko Iwabu and Toshitaka Nakagawa for their skilful assistance.

Funding

This study was supported by a Grant-in-Aid for Scientific Research from the Japan Society for the Promotion of Science and Grant-in Aid for Young Scientists (B) and by the Specially Promoted Research (2009, 2010) from Kagawa University.

Supplementary material available online at
http://jcs.biologists.org/lookup/suppl/doi:10.1242/jcs.083881/-/DC1

References

Araki, N., Johnson, M. T. and Swanson, J. A. (1996). A role for phosphoinositide 3-kinase in the completion of macropinocytosis and phagocytosis by macrophages. *J. Cell Biol.* **135**, 1249-1260.

Araki, N., Hatae, T., Yamada, T. and Hirohashi, S. (2000). Actinin-4 is preferentially involved in circular ruffling and macropinocytosis in mouse macrophages: analysis by fluorescence ratio imaging. *J. Cell Sci.* **113**, 3329-3340.

Araki, N., Hatae, T., Furukawa, A. and Swanson, J. A. (2003). Phosphoinositide-3-kinase-independent contractile activities associated with Fcgamma-receptor-mediated phagocytosis and macropinocytosis in macrophages. *J. Cell Sci.* **116**, 247-257.

Araki, N., Egami, Y., Watanabe, Y. and Hatae, T. (2007). Phosphoinositide metabolism during membrane ruffling and macropinosome formation in EGF-stimulated A431 cells. *Exp. Cell Res.* **313**, 1496-1507.

Beemiller, P., Zhang, Y., Mohan, S., Levinsohn, E., Gaeta, I., Hoppe, A. D. and Swanson, J. A. (2010). A Cdc42 activation cycle coordinated by PI 3-kinase during Fc receptor-mediated phagocytosis. *Mol. Biol. Cell* **21**, 470-480.

Botelho, R. J., Teruel, M., Dierckman, R., Anderson, R., Wells, A., York, J. D., Meyer, T. and Grinstein, S. (2000). Localized biphasic changes in phosphatidylinositol-4,5-bisphosphate at sites of phagocytosis. *J. Cell Biol.* **151**, 1353-1368.

Braun, V., Fraisier, V., Raposo, G., Hurbain, I., Sibarita, J. B., Chavrier, P., Galli, T. and Niedergang, F. (2004). TI-VAMP/VAMP7 is required for optimal phagocytosis of opsonised particles in macrophages. *EMBO J.* **23**, 4166-4176.

Cannon, G. J. and Swanson, J. A. (1992). The macrophage capacity for phagocytosis. *J. Cell Sci.* **101**, 907-913.
Caron, E. and Hall, A. (1998). Identification of two distinct mechanisms of phagocytosis controlled by different Rho GTPases. *Science* **282**, 1717-1721.
Castellano, F., Montcourrier, P. and Chavrier, P. (2000). Membrane recruitment of Rac1 triggers phagocytosis. *J. Cell Sci.* **113**, 2955-2961.
Castellano, F., Le Clainche, C., Patin, D., Carlier, M. F. and Chavrier, P. (2001). A WASp-VASP complex regulates actin polymerization at the plasma membrane. *EMBO J.* **20**, 5603-5614.
Chevallier, J., Koop, C., Srivastava, A., Petrie, R. J., Lamarche-Vane, N. and Presley, J. F. (2009). Rab35 regulates neurite outgrowth and cell shape. *FEBS Lett.* **583**, 1096-1101.
Coppolino, M. G., Krause, M., Hagendorff, P., Monner, D. A., Trimble, W., Grinstein, S., Wehland, J. and Sechi, A. S. (2001). Evidence for a molecular complex consisting of Fyb/SLAP, SLP-76, Nck, VASP and WASP that links the actin cytoskeleton to Fcgamma receptor signalling during phagocytosis. *J. Cell Sci.* **114**, 4307-4318.
Cox, D., Chang, P., Zhang, Q., Reddy, P. G., Bokoch, G. M. and Greenberg, S. (1997). Requirements for both Rac1 and Cdc42 in membrane ruffling and phagocytosis in leukocytes. *J. Exp. Med.* **186**, 1487-1494.
Cox, D., Tseng, C. C., Bjekic, G. and Greenberg, S. (1999). A requirement for phosphatidylinositol 3-kinase in pseudopod extension. *J. Biol. Chem.* **274**, 1240-1247.
Downey, G. P., Botelho, R. J., Butler, J. R., Moltyaner, Y., Chien, P., Schreiber, A. D. and Grinstein, S. (1999). Phagosomal maturation, acidification, and inhibition of bacterial growth in nonphagocytic cells transfected with FcgammaRIIA receptors. *J. Biol. Chem.* **274**, 28436-28444.
Fukuda, M. (2008). Regulation of secretory vesicle traffic by Rab small GTPases. *Cell Mol. Life Sci.* **65**, 2801-2813.
Greenberg, S. and Grinstein, S. (2002). Phagocytosis and innate immunity. *Curr. Opin. Immunol.* **14**, 136-145.
Grosshans, B. L., Ortiz, D. and Novick, P. (2006). Rabs and their effectors: achieving specificity in membrane traffic. *Proc. Natl. Acad. Sci. USA* **103**, 11821-11827.
Groves, E., Dart, A. E., Covarelli, V. and Caron, E. (2008). Molecular mechanisms of phagocytic uptake in mammalian cells. *Cell Mol. Life Sci.* **65**, 1957-1976.
Heo, W. D., Inoue, T., Park, W. S., Kim, M. L., Park, B. O., Wandless, T. J. and Meyer, T. (2006). PI(3,4,5)P3 and PI(4,5)P2 lipids target proteins with polybasic clusters to the plasma membrane. *Science* **314**, 1458-1461.
Higgs, H. N. and Pollard, T. D. (2001). Regulation of actin filament network formation through ARP2/3 complex: activation by a diverse array of proteins. *Annu. Rev. Biochem* **70**, 649-676.
Hoppe, A. D. and Swanson, J. A. (2004). Cdc42, Rac1, and Rac2 display distinct patterns of activation during phagocytosis. *Mol. Biol. Cell* **15**, 3509-3519.
Jackson, T. R., Brown, F. D., Nie, Z., Miura, K., Foroni, L., Sun, J., Hsu, V. W., Donaldson, J. G. and Randazzo, P. A. (2000). ACAPs are arf6 GTPase-activating proteins that function in the cell periphery. *J. Cell Biol.* **151**, 627-638.
Jordens, I., Marsman, M., Kuijl, C. and Neefjes, J. (2005). Rab proteins, connecting transport and vesicle fusion. *Traffic* **6**, 1070-1077.
Kanno, E., Ishibashi, K., Kobayashi, H., Matsui, T., Ohbayashi, N. and Fukuda, M. (2010). Comprehensive screening for novel rab-binding proteins by GST pull-down assay using 60 different mammalian Rabs. *Traffic* **11**, 491-507.
Kouranti, I., Sachse, M., Arouche, N., Goud, B. and Echard, A. (2006). Rab35 regulates an endocytic recycling pathway essential for the terminal steps of cytokinesis. *Curr. Biol.* **16**, 1719-1725.
Marshall, J. G., Booth, J. W., Stambolic, V., Mak, T., Balla, T., Schreiber, A. D., Meyer, T. and Grinstein, S. (2001). Restricted accumulation of phosphatidylinositol 3-kinase products in a plasmalemmal subdomain during Fc gamma receptor-mediated phagocytosis. *J. Cell Biol.* **153**, 1369-1380.
Massol, P., Montcourrier, P., Guillemot, J. C. and Chavrier, P. (1998). Fc receptor-mediated phagocytosis requires CDC42 and Rac1. *EMBO J.* **17**, 6219-6229.
May, R. C. and Machesky, L. M. (2001). Phagocytosis and the actin cytoskeleton. *J. Cell Sci.* **114**, 1061-1077.
May, R. C., Caron, E., Hall, A. and Machesky, L. M. (2000). Involvement of the Arp2/3 complex in phagocytosis mediated by FcgammaR or CR3. *Nat. Cell Biol.* **2**, 246-248.
Niedergang, F., Colucci-Guyon, E., Dubois, T., Raposo, G. and Chavrier, P. (2003). ADP ribosylation factor 6 is activated and controls membrane delivery during phagocytosis in macrophages. *J. Cell Biol.* **161**, 1143-1150.
Park, H. and Cox, D. (2009). Cdc42 Regulates Fc{gamma} receptor-mediated phagocytosis through the activation and phosphorylation of WASP and N-WASP. *Mol. Biol. Cell* **20**, 4500-4508.
Patino-Lopez, G., Dong, X., Ben-Aissa, K., Bernot, K. M., Itoh, T., Fukuda, M., Kruhlak, M. J., Samelson, L. E. and Shaw, S. (2008). Rab35 and its GAP EPI64C in T cells regulate receptor recycling and immunological synapse formation. *J. Biol. Chem.* **283**, 18323-18330.
Pereira-Leal, J. B. and Seabra, M. C. (2001). Evolution of the Rab family of small GTP-binding proteins. *J. Mol. Biol.* **313**, 889-901.
Sato, M., Sato, K., Liou, W., Pant, S., Harada, A. and Grant, B. D. (2008). Regulation of endocytic recycling by C. elegans Rab35 and its regulator RME-4, a coated-pit protein. *EMBO J.* **27**, 1183-1196.
Schwartz, S. L., Cao, C., Pylypenko, O., Rak, A. and Wandinger-Ness, A. (2007). Rab GTPases at a glance. *J. Cell Sci.* **120**, 3905-3910.
Scott, C. C., Dobson, W., Botelho, R. J., Coady-Osberg, N., Chavrier, P., Knecht, D. A., Heath, C., Stahl, P. and Grinstein, S. (2005). Phosphatidylinositol-4,5-bisphosphate hydrolysis directs actin remodeling during phagocytosis. *J. Cell Biol.* **169**, 139-149.
Shim, J., Lee, S. M., Lee, M. S., Yoon, J., Kweon, H. S. and Kim, Y. J. (2010). Rab35 mediates transport of Cdc42 and Rac1 to the plasma membrane during phagocytosis. *Mol. Cell Biol.* **30**, 1421-1433.
Smith, A. C., Heo, W. D., Braun, V., Jiang, X., Macrae, C., Casanova, J. E., Scidmore, M. A., Grinstein, S., Meyer, T. and Brumell, J. H. (2007). A network of Rab GTPases controls phagosome maturation and is modulated by Salmonella enterica serovar Typhimurium. *J. Cell Biol.* **176**, 263-268.
Stenmark, H. (2009). Rab GTPases as coordinators of vesicle traffic. *Nat. Rev. Mol. Cell Biol.* **10**, 513-525.
Swanson, J. A. (2008). Shaping cups into phagosomes and macropinosomes. *Nat. Rev. Mol. Cell Biol.* **9**, 639-649.
Swanson, J. A. and Hoppe, A. D. (2004). The coordination of signaling during Fc receptor-mediated phagocytosis. *J. Leukoc. Biol.* **76**, 1093-1103.
Takenawa, T. and Miki, H. (2001). WASP and WAVE family proteins: key molecules for rapid rearrangement of cortical actin filaments and cell movement. *J. Cell Sci.* **114**, 1801-1809.
Vieira, O. V., Botelho, R. J., Rameh, L., Brachmann, S. M., Matsuo, T., Davidson, H. W., Schreiber, A., Backer, J. M., Cantley, L. C. and Grinstein, S. (2001). Distinct roles of class I and class III phosphatidylinositol 3-kinases in phagosome formation and maturation. *J. Cell Biol.* **155**, 19-25.
Vieira, O. V., Botelho, R. J. and Grinstein, S. (2002). Phagosome maturation: aging gracefully. *Biochem J.* **366**, 689-704.
Yeung, T., Ozdamar, B., Paroutis, P. and Grinstein, S. (2006). Lipid metabolism and dynamics during phagocytosis. *Curr. Opin. Cell Biol.* **18**, 429-437.
Zerial, M. and McBride, H. (2001). Rab proteins as membrane organizers. *Nat. Rev. Mol. Cell Biol.* **2**, 107-117.
Zhang, J., Fonovic, M., Suyama, K., Bogyo, M. and Scott, M. P. (2009). Rab35 controls actin bundling by recruiting fascin as an effector protein. *Science* **325**, 1250-1254.
Zhang, Q., Cox, D., Tseng, C. C., Donaldson, J. G. and Greenberg, S. (1998). A requirement for ARF6 in Fcgamma receptor-mediated phagocytosis in macrophages. *J. Biol. Chem.* **273**, 19977-19981.